Atomistic Molecular Dynamic Simulations of Multiferroics

Dawei Wang, Jeevaka Weerasinghe, and L. Bellaiche

Phys. Rev. Lett. **109**, 067203 — Published 8 August 2012

DOI: 10.1103/PhysRevLett.109.067203

Atomistic Molecular Dynamic Simulations of Multiferroics

Dawei Wang,[1,2] Jeevaka Weerasinghe,[2] and L. Bellaiche[2,3]

[1]*Electronic Materials Research Laboratory - Key Laboratory of the Ministry of Education, and International Center for Dielectric Research, Xi'an Jiaotong University, Xi'an 710049, China*[*]
[2]*Physics department, University of Arkansas, Fayetteville, Arkansas 72701, USA*
[3]*Institute for Nanoscience and Engineering, University of Arkansas, Fayetteville, Arkansas 72701, USA*

A first-principles-based approach is developed to simulate *dynamical* properties, including complex permittivity and permeability in the GHz-THz range, of multiferroics at finite temperatures. It includes both structural degrees of freedom and magnetic moments as dynamic variables in Newtonian and Landau-Lifshitz-Gilbert (LLG) equations within molecular dynamics, respectively, with the *couplings* between these variables being incorporated. The use of a damping coefficient and of the fluctuation field in the LLG equations is required to obtain equilibrated magnetic properties at any temperature. No electromagnon is found in the spin-canted structure of of $BiFeO_3$. On the other hand, two magnons with very different frequencies are predicted via the use of this method. The smallest-in-frequency magnon corresponds to oscillations of the weak ferromagnetic vector in the basal plane being perpendicular to the polarization, while the second magnon corresponds to magnetic dipoles going in-and-out of this basal plane. The large value of the frequency of this second magnon is caused by *static* couplings between magnetic dipoles with electric dipoles and oxygen octahedra tiltings.

PACS numbers: 75.85.+t 31.15.xv 76.50.+g 75.30.Gw 76.60.Jx

Multiferroics form a promising class of materials exhibiting a rare coexistence between ferroelectricity and magnetism. They are experiencing a huge regain in interest, partly for designing novel advanced technologies (see, e.g., Refs. [1, 2] and references therein). The development and use of *ab-initio* atomistic schemes recently had helped in gaining a better knowledge of these complex materials. For instance, first-principles-based simulations explained why so few compounds are multiferroics [3] and how their magnetic ordering can be controlled by the application of electric fields along specific directions [4–7]. They also provided a deep insight into the strain-driven phase transition towards states with giant axial ratio and large out-of-plane polarization in $BiFeO_3$ (BFO) multiferroics [8–11]. Similarly, *ab-initio* techniques revealed that a dramatic enhancement of magnetoelectric coefficients can be achieved near this latter phase transition [12, 13]. Another example is the prediction of array of ferroelectric (FE) vortices in BFO films [14] – that was then experimentally confirmed [15]. Interestingly, all these latter breakthroughs from first principles concerned *static* properties of multiferroics. On the other hand, one particularly challenging issue that remains to be tackled by atomistic methods, in general, and by first-principles techniques, in particular, is the prediction of *dynamical* properties of multiferroics at finite temperature. One particular reason behind such lack of numerical tool is that ionic variables (e.g., polarization and/or tilting of oxygen octahedra) obey Newton's equations of motion while the spin degrees of freedom do not (such latter degrees of freedom follow Landau-Lifshitz [16] or even more complicated equations such as Landau-Lifshitz-Gilbert (LLG) [17]). In order to realistically mimic dynamical properties of multiferroics, one thus needs to develop a tool where different equations are simultaneously obeyed, and that also includes the coupling between ionic and magnetic variables. Moreover and in order to predict *finite-temperature* dynamics of multiferroics, this hypothetical tool should also be able to control (at the same time) the temperature associated with ionic motions *and* the temperature associated with magnetic degrees of freedom. Such simultaneously control is not an easy task to accomplish. On the other hand, developing such code can be of large benefits. For instance, it may help in understanding what is the nature of the excitation, having a frequency that is larger than typical magnon frequencies but smaller than phonon frequencies, that has been recently observed in BFO systems (see Ref. [18] and Fig. 2 of Ref. [19] for the "mysterious" excitation having a frequency of the order of 30-60 cm^{-1}). Can it be an electromagnon [20–22], as suggested in Ref. [18]?

The purpose of this Letter is to demonstrate that it is possible to develop such an *ab-initio* scheme, and to apply it to the study of BFO. It is found that LLG equations, in which a realistic damping coefficient is used and in which a fluctuation field is incorporated, coupled with classical Newtonian equations allow to reach the equilibrium states of both the structural and magnetic variables at any temperature. The use of this tool also yields the computation of the complex electric and magnetic susceptibilities for any frequency in the GHz-THz range. In particular, it predicts that the aforementioned mysterious excitation is in fact a magnon rather than an electromagnon, and that its large frequency originates from static (rather than dynamic) couplings between the magnetic dipoles with electric dipoles and oxygen octahedra tilting.

Here, we first take advantage of the first-principles-based effective Hamiltonian developed for BFO systems [23, 24]. Its total internal energy, E_{tot}, is written as a sum of two main terms:

$$\begin{aligned} E_{\text{tot}} =& E_{\text{FE-AFD}}(\{\boldsymbol{u}_i\},\{\eta\},\{\boldsymbol{\omega}_i\}) \\ &+ E_{\text{MAG}}(\{\boldsymbol{m}_i\},\{\boldsymbol{u}_i\},\{\eta\},\{\boldsymbol{\omega}_i\}), \end{aligned} \tag{1}$$

where $\boldsymbol{u}_i$ is the local soft mode in unit cell i, which is directly proportional to the electrical dipole centered on that cell. $\{\eta\}$ is the strain tensor, and contains both homogeneous and inhomogeneous parts [25, 26]. The $\boldsymbol{\omega}_i$ pseudo-vector characterizes the oxygen octahedra tilt, that is also termed the antiferrodistortive (AFD) motion, in unit cell i [23]. $\boldsymbol{m}_i$ is the magnetic dipole moment centered on the Fe-site i and has a fixed magnitude of $4\mu_B$ [27]. $E_{\text{FE-AFD}}$ is given in Ref. [28] and involves terms associated with ferroelectricity, strain and AFD motions, and their mutual couplings. E_{MAG} gathers magnetic degrees of freedom and their couplings, and is given in Refs. [23, 24]. Note that the use of this effective Hamiltonian approach within *Monte-Carlo* (MC) simulations was shown to (i) correctly yield the $R3c$ ground state that exhibits a coexistence of a spontaneous polarization with antiphase oxygen octahedra tilt in BFO bulks [23]; (ii) provide accurate Neel and Curie temperatures, and intrinsic magnetoelectric coefficients in BFO bulks and thin films [13, 23, 29]; and also (iii) reproduces the spin-canted magnetic structure that is characterized by a weak magnetization superimposed on a large G-type antiferromagnetic (AFM) vector in BFO films (Note that this spin-canted structure originated from the AFD motions rather than the polarization) [24]. Note, however, that the current version of this effective Hamiltonian approach does not yield a spin cycloid structure in BFO bulks, unlike in experiments [20]. The probable reason for that is either the lack of an additional energetic term that generates such cycloid or that the period of the cycloid [20] is too large to be mimicked by atomistic simulations. The present results should thus be relevant to BFO thin films (for which no cycloid exists) [30, 31].

Here, we decided to combine the effective Hamiltonian scheme within an original *Molecular Dynamics* (MD) scheme, in order to be able to predict *dynamical* properties. Technically, and as done in References [32, 33, 35], Newtonian equations are implemented for the $\{\boldsymbol{u}_i\}, \{\eta\}, \{\boldsymbol{\omega}_i\}$ variables, with the corresponding forces appearing in these equations having been obtained by taking partial differential of the E_{tot} energy of Eq. (1) with respect to each variable. As also previously implemented [32, 33], the temperatures of these lattice variables are controlled by Evans-Hoover thermostats [36]. The novelty here is to also include the dynamics of the magnetic moments on the same footing than the dynamics of the structural variables at a given temperature (note that we are not aware of any previous study addressing such simultaneous "double" dynamics, and that controlling temperature for the magnetic sublattice is a challenging problem [17, 37, 38]). For that, we implemented the stochastic Landau-Lifshitz-Gilbert (LLG) equation [17] for the $\boldsymbol{m}_i$'s degrees of freedom:

$$\begin{aligned}\frac{d\boldsymbol{m}_i}{dt} =& -\gamma \boldsymbol{m}_i \times \left[\boldsymbol{B}^i_{\text{eff}}(t) + \boldsymbol{b}^i_{\text{fl}}(t)\right] \\ & - \gamma \frac{\lambda}{|\boldsymbol{m}_i|(1+\lambda^2)} \boldsymbol{m}_i \times \left\{\boldsymbol{m}_i \times \left[\boldsymbol{B}^i_{\text{eff}}(t) + \boldsymbol{b}^i_{\text{fl}}(t)\right]\right\},\end{aligned} \tag{2}$$

where $\boldsymbol{B}^i_{\text{eff}} = -\partial E_{\text{tot}}/\partial \boldsymbol{m}_i$ is the effective magnetic field acting on the ith magnetic moment, γ is the gyromagnetic ratio, λ is the damping coefficient and $\boldsymbol{b}^i_{\text{fl}}$ is a fluctuation field that also acts on the ith magnetic moment. As we will see below, the introduction of this latter fluctuation field is crucial to obtain correct magnetic properties in a multiferroic at finite temperature, as consistent with previous studies done on magnetic systems [39, 40]. Technically, we use the Box-Muller method (that generates Gaussian distributed numbers for each magnetic moment) to simulate $\boldsymbol{b}^i_{\text{fl}}$ and to enforce the following conditions to be obeyed by this fluctuation field at the finite temperature, T [17, 39]:

$$\left\langle \boldsymbol{b}^i_{\text{fl}} \right\rangle = 0, \tag{3}$$

$$\left\langle b^i_{\text{fl},\alpha}(t_1)\, b^i_{\text{fl},\beta}(t_2) \right\rangle = 2\frac{\lambda k_B T}{\gamma |\boldsymbol{m}_i|}\delta_{\alpha,\beta}\delta(t_1 - t_2), \tag{4}$$

where α and β denote Cartesian coordinates and t_1 and t_2 are two different times. $\langle\rangle$ indicates an average over possible realizations of the fluctuating field [17], $\delta_{\alpha,\beta}$ is Kronecker delta function and $\delta(t_1 - t_2)$ is a Dirac delta function. A semi-implicit method devised by Mentink *et al* [41] is adopted here to (i) properly integrate the LLG equation, which is a Stratonovich stochastic differential equation [17] (the need to properly integrate LLG equation is a pivotal point that has been discussed in several studies [17, 41–45]); and (ii) to enforce the conservation of the magnetic moments' magnitude. The Mentink algorithm is efficient by limiting the matrix inversion procedure – which is needed by an implicit integrator – for each magnetic moment at each time step. We have checked that this algorithm indeed conserves the magnitude of the individual magnetic moments very well, and satisfies our need for efficiency and stability. Simulations on a periodic $12 \times 12 \times 12$ supercell (8,640 atoms) are performed within the presently developed MD scheme to obtain finite-temperature properties of BFO. The system is first equilibrated at a chosen temperature and pressure (NPT ensemble), and then, depending on the purpose of the simulation, we either continue having NPT steps to extract static properties, or adopt NVE steps to obtain time-resolved properties, such as autocorrelation functions of electric or magnetic dipoles, to predict dynamical properties. A time step of 0.5 fs is used in all simulations.

One important problem to address when dealing with dynamics of magnetic degrees of freedom and the LLG equation is to determine the *realistic* value, or range of values, of the damping coefficient for a given system. One way to solve such problem is to realize that MC and MD should give identical results for *static* properties at any temperature. As a result, MC can be used as a way of gauging MD simulations, and extracting the proper damping constant λ [46]. We numerically found that, at any temperature, λ has little effect on the spontaneous polarization and oxygen octahedra tilting, therefore yielding MD results being similar to the MC predictions for these structural properties for a wide range of damping coefficients. In fact, the effect of λ can be clearly seen when investigating *magnetic* properties in the multiferroic BFO – as consistent with the fact that λ "only" appears in the spin equations

of motions. Consequently, Fig. 1 shows the temperature evolution of the L magnitude of the G-type AFM vector for different λ values within the MD scheme, as well as, the MC prediction for such quantity. Moreover, parts (a) and (b) of this figure display the results when the fluctuation field is neglected and accounted for, respectively, in the MD simulations, in order to also reveal the importance of $\boldsymbol{b}_{\text{fl}}^{i}$ on finite-temperature magnetism. One can see that, without the fluctuation field, (i) MD simulations with $\lambda \gtrsim 1.0\times10^{-4}$ give an AFM vector that is significantly larger than that from the use of the MC technique for any temperature ranging between 10 K and 800 K, and therefore also generates a larger Neel temperature; while (ii) for damping coefficients smaller than 1.0×10^{-4} (including the case of $\lambda = 0$), the MD results are consistent with the MC calculations for temperatures larger than 250 K but yield too small AFM vectors for lower temperatures [47]. Therefore, not a single proper λ value allowing the MD simulations of the AFM vector to match the MC results across all temperatures can be found without a fluctuation field. On the other hand, Fig. 1 (b) demonstrates that a wide range of λ (namely, $1.0 \times 10^{-4} \leq \lambda \leq 1.0 \times 10^{-1}$) leads to a satisfactory agreement (i.e., a difference of less than 3%) between the MD and MC results at any temperature, *when the fluctuation field is included*. Such results thus prove the crucial importance of a fluctuation field for accurately modelling finite-temperature spin dynamics in multiferroics. Note also that a large range of λ can be adopted to obtain equilibrated static properties, which makes the MD approach suitable to model different multiferroic/ferromagnetic bulks or nanostructures that may have very different damping constants due to different damping mechanisms [48].

Let us now use the proposed MD scheme, incorporating the fluctuation field and choosing $\lambda = 1.0\times10^{-4}$, to compute the complex electric and magnetic susceptibilities of BFO, to be denoted by χ_e and χ_m, respectively. Such quantities can be calculated as follows [32, 49, 50]:

$$[\chi_e(\nu)]_{\alpha\beta} = \frac{1}{\varepsilon_0 V k_B T}\left[\langle d_\alpha(t) d_\beta(t)\rangle + i2\pi\nu\int_0^\infty dt e^{i2\pi\nu t}\langle d_\alpha(t)\, d_\beta(0)\rangle\right], \quad (5)$$

$$[\chi_m(\nu)]_{\alpha\beta} = \frac{\mu_0}{V k_B T}\left[\langle M_\alpha(t) M_\beta(t)\rangle + i2\pi\nu\int_0^\infty dt e^{i2\pi\nu t}\langle M_\alpha(t)\, M_\beta(0)\rangle\right], \quad (6)$$

where ν is the frequency while α and β define Cartesian components – with the x, y and z axes being along the pseudo-cubic [100], [010] and [001] directions, respectively. $\boldsymbol{d}(t)$ and $\boldsymbol{M}(t)$ are the electric and magnetic dipole moments at time t, respectively. Here, we focus on a fixed temperature of 20 K, for which the crystallographic equilibrium state is $R3c$.

Figure 2 (a) shows the isotropic value of the $[\chi_e(\nu)]_{\alpha,\beta}$ dielectric response, that is $\left\{[\chi_e(\nu)]_{xx} + [\chi_e(\nu)]_{yy} + [\chi_e(\nu)]_{zz}\right\}/3$. Four peaks can be distinguished, having resonant frequencies of $151\,\text{cm}^{-1}$, $176\,\text{cm}^{-1}$, $240\,\text{cm}^{-1}$ and $263\,\text{cm}^{-1}$. They correspond to E, A_1, E and A_1 symmetries, respectively [51] Not all the modes appearing in measured Raman or infrared spectra [19, 52–59] can be reproduced by our simulations because of the limited number of degrees of freedom included in the effective Hamiltonian. In particular, the modes observed around 74 and 81 cm^{-1}, and that are E(TO) and E(LO) modes, respectively, according to Ref. [59], are missing in our computations. Moreover, we numerically found that the first two (lowest-in-frequency) peaks of Fig. 2(a) are mostly related to the sole FE degree of freedom incorporated in the effective Hamiltonian scheme, while the last two peaks have also a significant contribution from AFD distortions – as consistent with Ref. [60]. As revealed in Refs. [33, 34], bilinear couplings between the FE and AFD modes in the $R3c$ phase allow the AFD mode to acquire some polarity, which explains why these last two peaks emerge in the dielectric spectra.

Regarding the permeability, *two* peaks can be seen in Fig. 2(b). Their predicted resonant frequencies are $\sim 7\,\text{cm}^{-1}$ and $\sim 85\,\text{cm}^{-1}$, respectively [61] Since none of the frequencies coincides with the dielectric resonant frequencies shown in Fig. 2(a), we can safely conclude that they are not electromagnons. They are rather "solely" magnons. Interestingly, we further numerically found that the lowest-in-frequency magnon entirely *disappears* when we switch off in our simulations the parameter responsible for the spin-canted structure of BFO. In other words, the purely AFM G-type structure does not possess such magnon. Moreover, the video shown in the Supplementary material S1 demonstrates that this magnon is associated with the rotation of magnetic dipoles *inside* the (111) plane (that contains the polarization). In other words, this magnon is the low-in-frequency excitation (possessing a gap) that has been predicted in Refs. [62, 63], and that corresponds to the oscillation of the weak ferromagnetic moment about its equilibrium position in the basal plane [64]. Let us now try to understand the origin of the second magnetic peak, for which the frequency is much larger than those of typical magnons (that are usually lower than 20 cm^{-1}) but is smaller than the phonon frequencies shown in Fig. 2a (this second peak is thus consistent with the "mysterious" excitations observed in Refs. [18, 19]. This second magnetic peak is associated with fast oscillations of the magnetic dipoles going *in-and-out* of the (111) plane, as well as, a change in length of the weak FM vector (see video in Supplementary material S1). This second peak therefore corresponds to the so-called optic antiferromagnetic mode of Ref. [65] and to the high-frequency gapped mode of Ref. [63]. Interestingly, we also numerically found that this second peak (i) has a resonant frequency that is insensitive to the effective masses associated with the FE and AFD motions (in other words, the frequency of this second magnetic peak is insensitive to a change of FE or AFD resonances); and (ii) becomes a broad peak ranging from 0 cm^{-1} to $\simeq 16\,\text{cm}^{-1}$ when switching off the coupling parameters between magnetic moments with FE and AFD motions in our simulations (in that case, the corresponding mo-

tions of the magnetic dipoles are not only in-and-out of the (111) plane but also are within the (111) plane). As a result, we can safely conclude that the abnormally large frequency of the second peak results from *static* (rather than dynamic) couplings between the $\boldsymbol{m}_i$'s and structural variables, with these couplings generating a large magnetic anisotropy. Furthermore, this second peak has a resonant frequency of around 60 cm^{-1} rather than$\sim 85\,\mathrm{cm}^{-1}$, if one "only" switches off the static coupling between magnetic degrees of freedom and AFD motions. In other words, AFD distortions (that have not been *explicitly* incorporated in phenomenological models so far to study dynamics of BFO systems) do significantly affect the resonant frequency of this second peak. Analytical expressions derived in the Supplementary material S2 from energetic terms included in the effective Hamiltonian confirm and even shed more light on such features, such as revealing that the resonant frequency of this second magnetic peak also depends on the values of the spontaneous polarization and angle of oxygen octahedra tilting [69]. We thus hope that our proposed atomistic MD method is, and will be, of large benefits to gain a deeper knowledge of the fascinating multiferroic materials [70]. Note that it can also open the door to many exciting studies, such as the computation and understanding of the cross-coupled electromagnetic susceptibility defined in Ref. [65].

Discussions with J. Iñiguez, Dr Kamba, M. Cazayous and M. Bibes are greatly acknowledged. We mostly thank Office of Basic Energy Sciences, under contract ER-46612 for personnel support. NSF grant DMR-0701558 and DMR-1066158, and ONR Grants N00014-11-1-0384 and N00014-08-1-0915 are also acknowledged for discussions with scientists sponsored by these grants. D.W. acknowledges support from the National Natural Science Foundation of China under Grant No. 10904122. Some computations were also made possible thanks to the MRI grant 0959124 from NSF, and N00014-07-1-0825 (DURIP) from ONR.

* Electronic address: dawei.wang@mail.xjtu.edu.cn

[1] T. Choi, S. Lee, Y. J. Choi, V. Kiryukhin, and S.-W. Cheong, Science **324**, 63 (2009).
[2] S. Y. Yang, J. Seidel, S. J. Byrnes, P. Shafer, C.-H. Yang, M. D. Rossell, P. Yu, Y.-H. Chu, J. F. Scott, J. W. Ager, L. W. Martin, and R. Ramesh, Nat. Nanotechnol. **5**, 143 (2010).
[3] N. Hill, J. Phys. Chem. B **104**, 6694 (2000).
[4] T. Zhao, A. Scholl, F. Zavaliche, K. Lee, M. Barry, A. Doran, M. P. Cruz, Y. H. Chu, C. Ederer, N. A. Spaldin, R. R. Das, D. M. Kim, S. H. Baek, C. B. Eom, and R. Ramesh, Nat. Mater. **5**, 823 (2006).
[5] D. Lebeugle, D. Colson, A. Forget, M. Viret, A. M. Bataille, and A. Gukasov, Phys. Rev. Lett. **100**, 227602 (2008).
[6] S. Lee, T. Choi, W. Ratcliff, R. Erwin, S.-W. Cheong, and V. Kiryukhin, Phys. Rev. B **78**, 100101(R) (2008).
[7] S. Lisenkov, D. Rahmedov, and L. Bellaiche, Phys. Rev. Lett. **103**, 047204 (2009).
[8] H. Béa, B. Dupé, S. Fusil, R. Mattana, E. Jacquet, B. Warot-Fonrose, F. Wilhelm, A. Rogalev, S. Petit, V. Cros, A. Anane, F. Petroff, K. Bouzehouane, G. Geneste, B. Dkhil, S. Lisenkov, I. Ponomareva, L. Bellaiche, M. Bibes, and A. Barthélémy, Phys. Rev. Lett. **102**, 217603 (2009).
[9] A. J. Hatt, N. A. Spaldin, and Claude Ederer, Phys. Rev. B **81**, 054109 (2010).
[10] R. J. Zeches, M. D. Rossell, J. X. Zhang, A. J. Hatt, Q. He, C.-H. Yang, A. Kumar, C. H. Wang, A. Melville, C. Adamo, G. Sheng, Y.-H. Chu, J. F. Ihlefeld, R. Erni, C. Ederer, V. Gopalan, L. Q. Chen, D. G. Schlom, N. A. Spaldin, L. W. Martin, and R. Ramesh, Science **326**, 977 (2009).
[11] B. Dupé, I. C. Infante, G. Geneste, P.-E. Janolin, M. Bibes, A. Barthélémy, S. Lisenkov, L. Bellaiche, S. Ravy, and B. Dkhil, Phys. Rev. B **81**, 144128 (2010).
[12] J. C. Wojdeł and J. Íñiguez, Phys. Rev. Lett. **105**, 037208 (2010).
[13] S. Prosandeev, I. A. Kornev, and L. Bellaiche, Phys. Rev. B **83**, 020102(R) (2011).
[14] S. Prosandeev, S. Lisenkov, and L. Bellaiche, Phys. Rev. Lett. **105**, 147603 (2010).
[15] C. Nelson, B. Winchester, Y. Zhang, and S. Kim, Nano Lett. **11**, 828 (2011).
[16] V. Antropov, S. Tretyakov, and B. Harmon, J. Appl. Phys. **81**, 3961 (1997).
[17] J. L. García-Palacios and F. J. Lázaro, Phys. Rev. B **58**, 14937 (1998)
[18] G. A. Komandin, V. I. Torgashev, A. A. Volkov, O. E. Porodinkov, I. E. Spektor, and A. A. Bush, Physics of the Solid State **52**, 734 (2010).
[19] S. Kamba, D. Nuzhnyy, M. Savinov, J. Šebek, J. Petzelt, J. Prokleška, R. Haumont, and J. Kreisel, Phys. Rev. B **75**, 024403 (2007).
[20] M. Cazayous, Y. Gallais, A. Sacuto, R. de Sousa, D. Lebeugle, and D. Colson, Phys. Rev. Lett. **101**, 037601 (2008).
[21] A. B. Sushkov, M. Mostovoy, R. Valdés Aguilar, S.-W. Cheong, and H. D. Drew, J. Phys.: Condens. Matter **20**, 434210 (2008).
[22] R. Valdés Aguilar, M. Mostovoy, A. Sushkov, C. Zhang, Y. Choi, S.-W. Cheong, and H. Drew, Phys. Rev. Lett. **102**, 047203 (2009).
[23] I. A. Kornev, S. Lisenkov, R. Haumont, B. Dkhil, and L. Bellaiche, Phys. Rev. Lett. **99**, 227602 (2007).
[24] D. Albrecht, S. Lisenkov, W. Ren, D. Rahmedov, I. A. Kornev, and L. Bellaiche, Phys. Rev. B **81**, 140401(R) (2010).
[25] W. Zhong, D. Vanderbilt, and K. M. Rabe, Phys. Rev. Lett. **73**, 1861 (1994).
[26] W. Zhong, D. Vanderbilt, and K. M. Rabe, Phys. Rev. B **52**, 6301 (1995).
[27] J. B. Neaton, C. Ederer, U. V. Waghmare, N. A. Spaldin, and K. M. Rabe, Phys. Rev. B **71**, 014113 (2005).
[28] I. A. Kornev, L. Bellaiche, P. E. Janolin, B. Dkhil, and E. Suard, Phys. Rev. Lett. **97**, 157601 (2006).
[29] I. Infante, S. Lisenkov, B. Dupé, M. Bibes, S. Fusil, E. Jacquet, G. Geneste, S. Petit, A. Courtial, J. Juraszek, L. Bellaiche, A. Barthélémy, and B. Dkhil, Phys. Rev. Lett. **105**, 057601 (2010).
[30] H. Bea, M. Bibes, A. Barthelemy, K. Bouzehouane, E. Jacquet, A. Khodan, J.-P. Contour, S. Fusil, F. Wyczisk, A. Forget, D. Lebeugle, D. Colson, and M. Viret, Appl. Phys. Lett. **87**, 072508 (2005).
[31] H. Bea, M. Bibes, S. Petit, J. Kreisel, and A. Barthelemy, Phil. Mag. Lett. **87**, 165 (2007).
[32] I. Ponomareva, L. Bellaiche, T. Ostapchuk, J. Hlinka, and J. Petzelt, Phys. Rev. B **77**, 012102 (2008).
[33] D. Wang, J. Weerasinghe, L. Bellaiche, and J. Hlinka, Phys.

Rev. B **83**, 020301(R) (2011).
[34] J. Weerasinghe, D. Wang and L. Bellaiche, Phys. Rev. B **85**, 014301 (2012).
[35] D. Wang, E. Buixaderas, J. Íñiguez, J. Weerasinghe, H. Wang, and L. Bellaiche, Phys. Rev. Lett. **107**, 175502 (2011).
[36] D. J. Evans, W. G. Hoover, B. H. Failor, B. Moran, and A. J. C. Ladd, Phys. Rev. A **28**, 1016 (1983).
[37] P.-W. Ma, C. H. Woo, and S. L. Dudarev, Phys. Rev. B **78**, 024434 (2008).
[38] P.-W. Ma, S. L. Dudarev, A. A. Semenov, and C. H. Woo, Phys. Rev. E **82**, 031111 (2010).
[39] W. Brown, Phys. Rev. **130**, 1667 (1963).
[40] R. Kubo and N. Hashitsume, Prog. Theor. Phys. Sup. **46**, 210 (1970).
[41] J. H. Mentink, M. V. Tretyakov, A. Fasolino, M. I. Katsnelson, and T. Rasing, J. Phys.: Condens. Matter **22**, 176001 (2010).
[42] W. E and X.-P. Wang, Siam J. Numer. Anal. **38**, 1647 (2000).
[43] T. Arponen and B. Leimkuhler, BIT Numer. Math. **44**, 403 (2004).
[44] M. Daquino, C. Serpico, and G. Miano, J. Comput. Phys. **209**, 730 (2005).
[45] I. Cimrák, Arch. Comput. Method. E. **15**, 277 (2008).
[46] B. Skubic, J. Hellsvik, L. Nordström, and O. Eriksson, J. Phys: Condens. Matter **20**, 315203 (2008).
[47] Item (ii) thus reveals that, at higher temperatures, the equilibrated lattice degrees of freedom in the system – local modes, AFD variables, strain tensor – act as a very good heat reservoir for the magnetic degrees of freedom even when no damping is included, but a too small damping prevents the magnetic sublattice from reaching its ground state at low temperatures.
[48] T. L. Gilbert, IEEE T. Magn. **40**, 3443 (2004).
[49] J. Caillol, D. Levesque, and J. Weis, J. Chem. Phys. **85**, 6645 (1986).
[50] J. Hlinka, T. Ostapchuk, D. Nuzhnyy, J. Petzelt, P. Kuzel, C. Kadlec, P. Vanek, I. Ponomareva, and L. Bellaiche, Phys. Rev. Lett. **101**, 167402 (2008).
[51] The phonon frequencies of BFO have been investigated using *ab-initio* computations [60, 67, 68] and Raman/infrared spectroscopy [19, 52–59]. Surprisingly, rather different results were obtained between these different studies, even for the modes' symmetry – in addition to the quantitative value of the resonant frequencies. As a result, Tutuncu et al [67] had assigned a margin of $40 - 50\,\mathrm{cm}^{-1}$ when comparing different results. Here, we have matched our MD results for the resonant frequencies and symmetry of the peaks to LDA+U phonon calculations of BFO in its $R3c$ phase, by tuning the effective masses of the FE and AFD modes.
[52] R. Haumont, J. Kreisel, P. Bouvier, and F. Hippert, Phys. Rev. B **73**, 132101 (2006).
[53] H. Fukumura, S. Matsui, H. Harima, T. Takahashi, T. Itoh, K. Kisoda, M. Tamada, Y. Noguchi, and M. Miyayama, J. Phys.: Condens. Matter **19**, 365224 (2007).
[54] R. P. S. M. Lobo, R. L. Moreira, D. Lebeugle, and D. Colson, Phys. Rev. B **76**, 172105 (2007).
[55] D. Rout, K.-S. Moon, and S.-J. L. Kang, J. Raman Spectrosc. **40**, 618 (2009).
[56] J. Lu, M. Schmidt, P. Lunkenheimer, A. Pimenov, A. A. Mukhin, V. D. Travkin, and A. Loidl, J. Phys.: Conf. Ser. **200**, 012106 (2010).
[57] R. Palai, H. Schmid, J. F. Scott, and R. S. Katiyar, Phys. Rev. B **81**, 064110 (2010).
[58] A. A. Porporati, K. Tsuji, M. Valant, A.-K. Axelsson, and G. Pezzotti, J. Raman Spectrosc. **41**, 84 (2010).
[59] J. Hlinka, J. Pokorny, S. Karimi, and I. M. Reaney, Phys. Rev. B **83**, 020101(R) (2011).
[60] P. Hermet, M. Goffinet, J. Kreisel, and P. Ghosez, Phys. Rev. B **75**, 220102(R) (2007).
[61] Note that we also computed the magnetic response associated with the G-type AFM vector, by replacing the magnetic dipole moments by the AFM ones in Eq. (6). We found that such AFM response has also two peaks, with their resonant frequencies coinciding with those of the permeability.
[62] P. Pincus, Phys. Rev. Lett. **5**, 13 (1960).
[63] R. de Souza and J.E. Moore, Appl. Phys. Lett. **92**, 022514 (2008).
[64] Note that switching off the parameter responsible for the spin-canting should shift down our lowest-in-frequency magnetic peak to 0 cm^{-1} [63]. We can not observe such resulting zero-frequency peak because our numerical technique can not efficiently probe frequencies lower than $\simeq 3$ cm^{-1} due to the picosecond time scale inherent to MD simulations.
[65] K. L. Livesey and R. L. Stamps, Phys. Rev. B **81**, 094405 (2010).
[66] C. Ederer and N. A. Spaldin, Phys. Rev. B **71**, 060401(R) (2005).
[67] H. Tütüncü, J. Appl. Phys. **103**, 083712 (2008).
[68] I. Apostolova, A. T. Apostolov, and J. M. Wesselinowa, J. Phys.: Condens. Matter **21**, 036002 (2009).
[69] Since the spontaneous polarization, angle of oxygen octahedra tiltings and, especially, magnetic-structural coupling parameters are rather difficult to be precisely determined from first principles, it is possible that the second magnon peak will be experimentally found at a different resonant frequency in BFO films (we are not aware of any published data reporting magnetic peaks in BFO films that do not possess magnetic cycloid). However, if future Raman or infrared measurements do confirm the existence of the electromagnon peak around $\sim 85\,\mathrm{cm}^{-1}$, one has to realize that it will nearly overlap with the E(LO) dielectric peak [59]. We also note that our MD simulations indicate that increasing the damping coefficient results in a decrease of the magnitude of the second magnetic peak.
[70] It is also important to realize that two main limitations are currently associated with the proposed method: (1) one can not study magnetic excitations associated with very low k-vectors because of the relatively small size of the supercell [63, 71]; and (2) excitations lower than $\simeq 3$ cm^{-1} can not be investigated because of the time scale of usual MD simulations. On the other hand, in addition to provide insightful atomistic details, our proposed scheme has also the advantage (with respect to phenomenological works) to extract its parameters from first principles. For instance, it provides an effective magnetic field associated with the parameter leading to spin canting (which is related to the coefficient K_{ij} in Eq. (1) of the supplemental material S2) of about 1 Tesla at low temperature. This value is about 7 times larger than the phenomenological value used in Ref. [65], which therefore questions the accuracy of this latter value since our K_{ij} parameter was shown to provide a weak ferromagnetic vector that agrees very well with experiment [24]. Our numerical tool also gives a Neel temperature of only $\simeq$ 150K if one neglects the static couplings between magnetic degrees of freedom and structural variables, to be compared with the value of $\simeq$ 660K when these couplings are included. Note that these latter couplings are those related to the E_{ij} and G_{ij} parameters of Eq. (1) of the supplemental material S2, since K_{ij} was found to have a negligible effect on the Neel temperature [24].
[71] A. K. Zvezdin and A. A. Mukhin, JETP Lett. **89**, 328 (2009).

Captions:

Figure 1: (Color online) Temperature dependency of the magnitude of the antiferromagnetic vector within the proposed MD scheme and for different damping coefficients, when the fluctuation field is neglected (Panel (a)) and incorporated (Panel (b)). For comparison, the MC results are also indicated by a red solid line.

Figure 2: (Color online) Complex electric (Panel (a)) and magnetic (Panel (b)) susceptibilities as a function of frequency in BFO at at $T = 20\,\mathrm{K}$.

Figure 3: (Color online) Sketch of the FM vector (green) and the L vector (red) at one instance. We note, at this instance, these two vectors slightly deviate from the (111) plane due to couplings with AFD and FE (see Supplementary information S2). The (weak) FM vector is enhanced by ~59 times to be seeable in this figure.

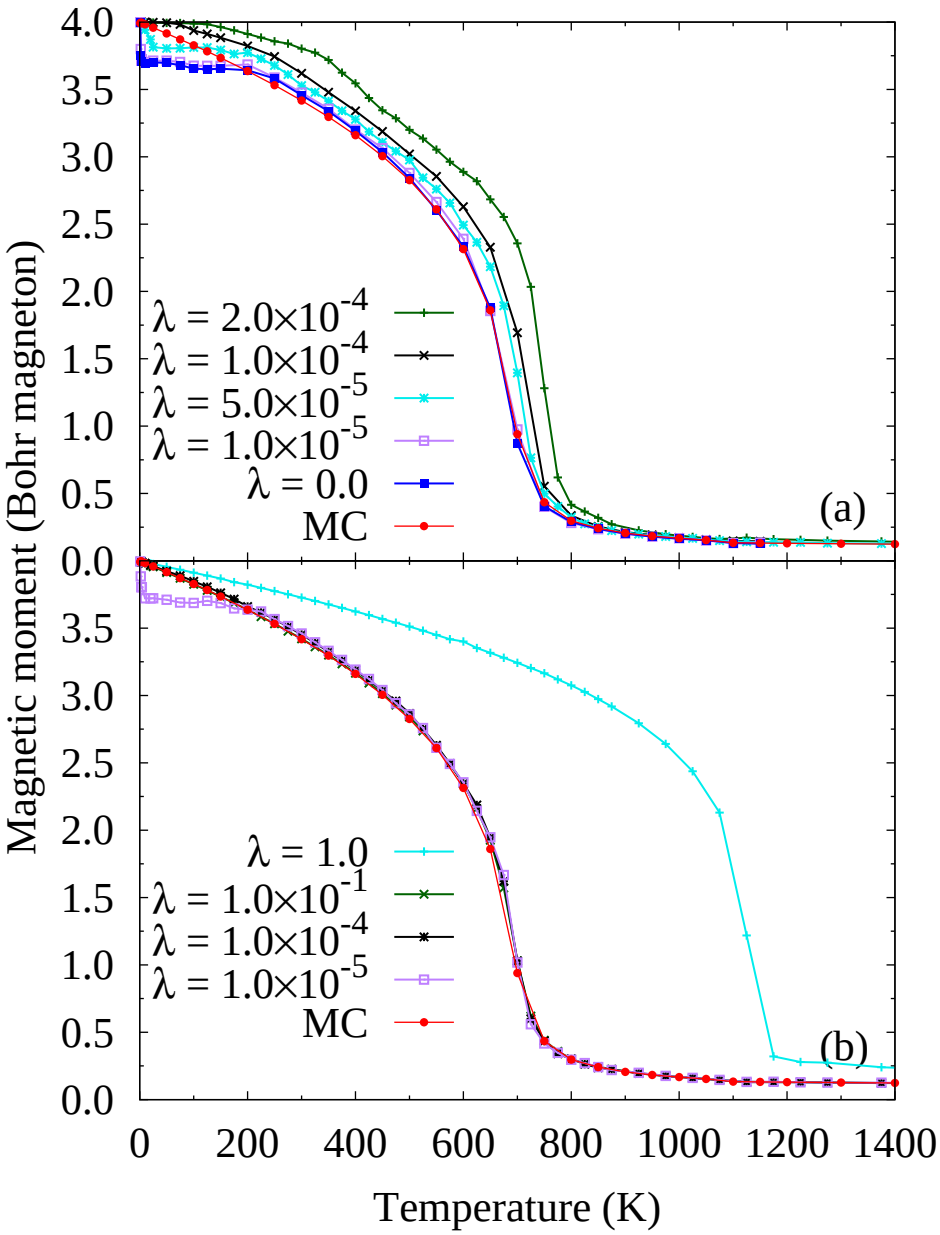

Figure 1 LK13183 10May2012

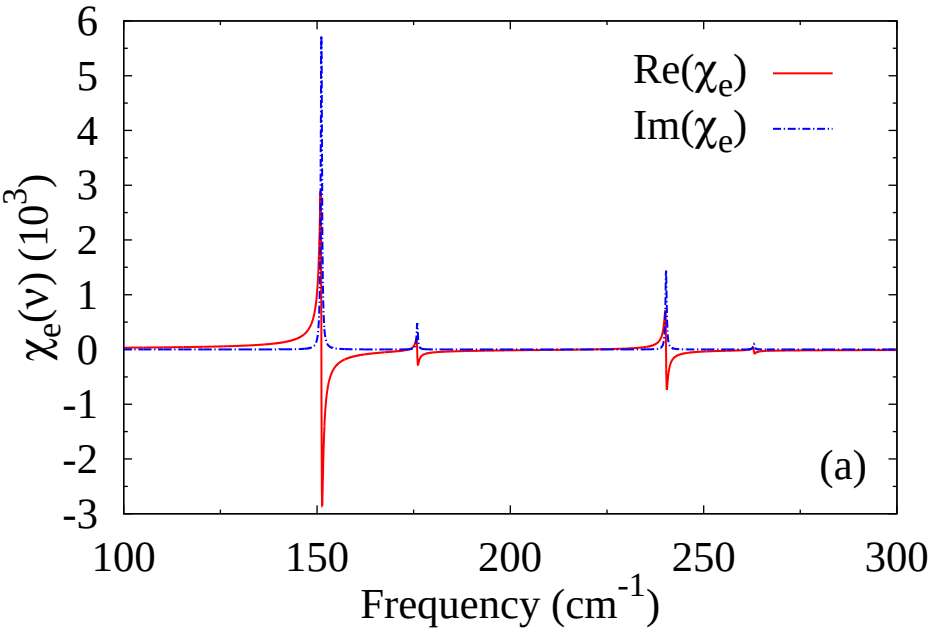

Figure 2a LK13183 10May2012

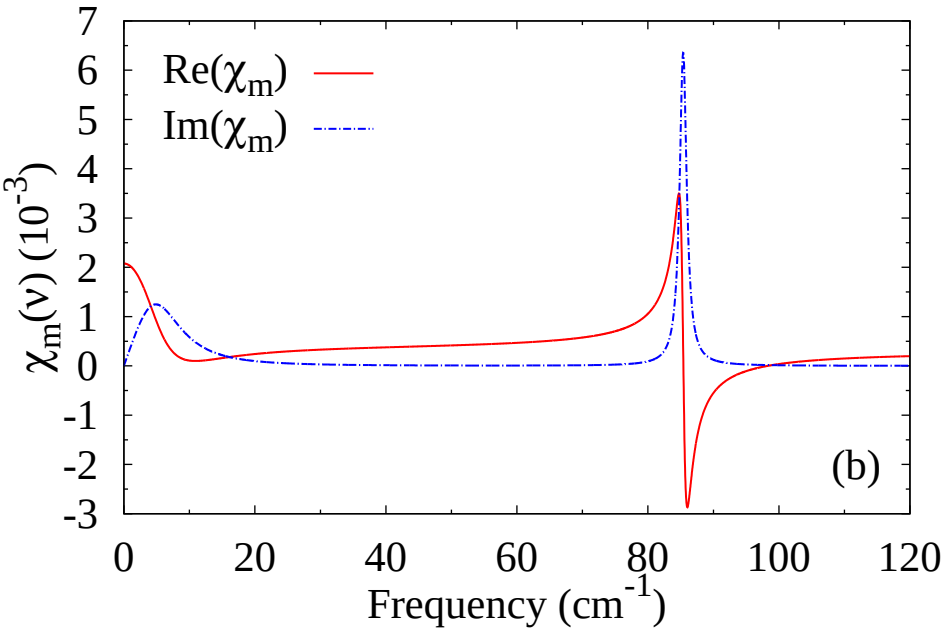

Figure 2b LK13183 10May2012

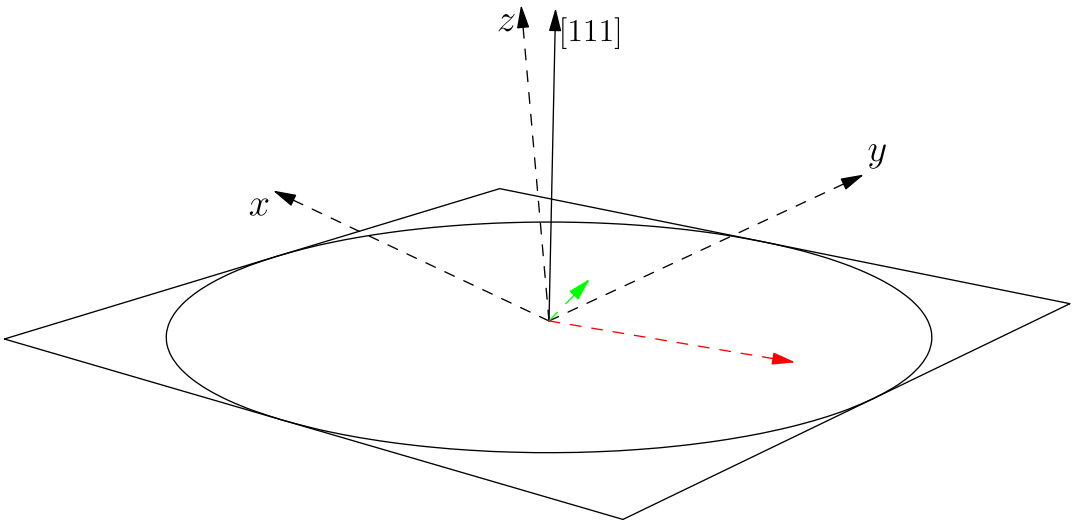

Figure 3 LK13183 10May2012